A Sphere Packing Bound for AWGN MIMO Fading Channels under Peak Amplitude Constraints

Antonino Favano*†, Marco Ferrari†, Maurizio Magarini*, and Luca Barletta*
*Politecnico di Milano, Milano, Italy, {antonino.favano, maurizio.magarini, luca.barletta}@polimi.it
†CNR-IEIIT, Milano, Italy, marco.ferrari@ieiit.cnr.it

***Abstract*—An upper bound on the capacity of multiple-input multiple-output (MIMO) additive white Gaussian noise fading channels is derived under peak amplitude constraints. The tightness of the bound is investigated at high signal-to-noise ratio (SNR), for any arbitrary convex amplitude constraint region. Moreover, a numerical simulation of the bound for fading MIMO channels is analyzed, at any SNR level, for a practical transmitter configuration employing a single power amplifier for all transmitting antennas.**

I. Introduction

The ever-growing requirements in data rates and the ubiquitous presence of wireless devices have made energy efficiency one of the fundamental features in the design of a wireless system, and power amplifiers are one of the main components that have a strong impact on its implementation. To properly exploit the available resources of a wireless channel, it is fundamental to establish a realistic information theoretic framework, providing an accurate estimate of attainable data rates. By imposing a communication under peak amplitude constraints at the input, one can accurately represent the limitations induced by the non-linear nature of power amplifiers. Some of the main results about channel capacity under peak amplitude constraints are presented in [1] and [2], where the authors consider scalar and quadrature Gaussian channels, respectively. Then, in [3] and [4] the capacity evaluation is extended to multiple-input multiple-output (MIMO) channels subject to a constraint that limits the norm of the input vector, while in [5] it is introduced a capacity evaluation for MIMO fading channels subject to any arbitrary peak amplitude constraint. Finally, in [6] we refined the results presented in [5] for two particular constraints of practical interest: one refers to a transmitter configuration employing multiple power amplifiers, one per transmitting antenna, while the other employs a single amplifier for all the antennas. Both constraints correspond to typical transmitter configurations in MIMO wireless communications, the latter being especially relevant in the case of massive MIMO systems.

Contribution

In this paper, we provide an asymptotically tight upper bound on the capacity of MIMO additive white Gaussian noise (AWGN) fading channels subject to peak amplitude constraints. We derive an upper bound by extending the results in [7] to MIMO systems, assuming perfect channel state information. We prove that the gap between the derived upper bound and the best lower bound found in the literature is asymptotically tight. Indeed, as the signal-to-noise ratio (SNR) goes to infinity, the bounds' gap vanishes for any channel matrix, any dimension of the MIMO system, and any convex constraint region. We also investigate the gap behavior versus the SNR in MIMO fading channels, for a particular transmitter configuration, inducing a constraint on the norm of the MIMO input vector.

In Section II, we introduce some useful mathematical tools needed throughout the rest of the paper, in Section III we define the system model, in Section IV we outline previous results present in the literature, and in Section V we propose a sphere packing (SP) upper bound and prove that it is asymptotically tight at high SNR. In Section VI, we apply the bound to a particular peak amplitude constraint, and finally Section VII concludes the paper.

Notation

We use bold letters for vectors ($\mathbf{x}$), uppercase letters for random variables (X), calligraphic uppercase letters for subsets of vector spaces ($\mathcal{X}$), and uppercase sans serif letters for matrices (H). We denote by H^T the transposed of a matrix H. Then, $\mathcal{CN}(\boldsymbol{\mu}, \Sigma)$ indicates a complex multivariate Gaussian distribution with mean vector $\boldsymbol{\mu}$ and covariance matrix Σ. We represent the $n \times 1$ vector of zeros by $\mathbf{0}_n$ and the $n \times n$ identity matrix by I_n. Moreover, we denote by $\mathcal{B}_n \triangleq \{\mathbf{x} : \|\mathbf{x}\| \leq 1\}$ the n-dimensional unit ball in $\mathbb{R}^n$ centered in $\mathbf{0}_n$, with volume $\pi^{\frac{n}{2}}/\Gamma\left(\frac{n}{2}+1\right)$, and $\delta\mathcal{B}_n \triangleq \{\mathbf{x} : \|\mathbf{x}\| \leq \delta\}$ as the n-dimensional ball of radius δ centered in $\mathbf{0}_n$. Finally, we define $\mathsf{H}\mathcal{X} \triangleq \{\mathbf{y} : \mathbf{y} = \mathsf{H}\mathbf{x}, \mathbf{x} \in \mathcal{X}\}$, with $[\mathsf{H}\mathcal{X}]^{\times M}$ the Cartesian product of $\mathsf{H}\mathcal{X}$ with itself M times, and with $\mathrm{Vol}_n(\mathcal{X})$ we indicate the n-dimensional volume of the set $\mathcal{X}$.

II. Preliminaries

Given two subsets $\mathcal{K}$ and $\mathcal{R}$ of a vector space, the Minkowski sum is denoted by the operator $\oplus$ and it gives the set obtained by adding each vector in $\mathcal{K}$ to each vector in $\mathcal{R}$

$$\mathcal{K} \oplus \mathcal{R} \triangleq \{\mathbf{k}+\mathbf{r} | \mathbf{k} \in \mathcal{K},\ \mathbf{r} \in \mathcal{R}\}. \quad (1)$$

Moreover, if $\mathcal{K}$ is a convex body of $\mathbb{R}^n$, we denote by $\mathrm{V}_j(\mathcal{K})$ the jth intrinsic volume of $\mathcal{K}$. The intrinsic volume represents a fundamental measure of content for a convex body [8]. Thanks to the Steiner's formula [7, Theorem 4] we can evaluate the n-dimensional volume of a Minkowski sum as follows

$$\mathrm{Vol}_n(\mathcal{K} \oplus \delta\mathcal{B}_n) = \sum_{j=0}^{n} \mathrm{V}_j(\mathcal{K})\, \mathrm{Vol}_{n-j}(\delta\mathcal{B}_{n-j}). \tag{2}$$

Since (2) is a convolution, it is useful to introduce the generating function of the intrinsic volumes of $\mathcal{K}$ as [7, Theorem 8]

$$G_{\mathcal{K}}(t) = \log\left(\sum_{j=0}^{n} \mathrm{V}_j(\mathcal{K})\, e^{jt}\right). \tag{3}$$

An important property of these generating functions is that given two sets $\mathcal{K}$ and $\mathcal{R}$, as shown in [8], it holds

$$G_{\mathcal{K}\times\mathcal{R}}(t) = G_{\mathcal{K}}(t) \cdot G_{\mathcal{R}}(t). \tag{4}$$

Finally, given a scalar function $f(t)$, we define the convex conjugate of $f(t)$ as

$$f^*(\theta) \triangleq \sup_t \{\theta t - f(t)\}. \tag{5}$$

III. System Model

Let us consider an $N \times N$ complex MIMO system with input-output relationship given by

$$\widetilde{\mathbf{Y}} = \widetilde{\mathsf{H}} \cdot \widetilde{\mathbf{X}} + \widetilde{\mathbf{Z}}. \tag{6}$$

The input vector $\widetilde{\mathbf{X}}$ is such that $\widetilde{\mathbf{X}} \in \widetilde{\mathcal{X}}$ with $\widetilde{\mathcal{X}}$ being a convex constraint region, $\widetilde{\mathbf{Z}} \sim \mathcal{CN}(\mathbf{0}_N, 2\sigma_z^2 \mathsf{I}_N)$ is the noise vector, and $\widetilde{\mathsf{H}}$ is any full rank channel fading matrix. We assume $\widetilde{\mathsf{H}}$ to be fixed throughout the channel uses and known both at the transmitter and at the receiver. Let us vectorize the system in (6) in its real and imaginary components. We obtain the equivalent model

$$\mathbf{Y} = \mathsf{H} \cdot \mathbf{X} + \mathbf{Z}, \tag{7}$$

with $\mathsf{H} = \mathrm{Re}\{\widetilde{\mathsf{H}}\} \otimes \mathsf{I}_2 + \mathrm{Im}\{\widetilde{\mathsf{H}}\} \otimes \left[\begin{smallmatrix} 0 & -1 \\ 1 & 0 \end{smallmatrix}\right]$, where the operator $\otimes$ is the Kronecker product, $\mathbf{Y}$ is an $2N \times 1$ vector defined as $\mathbf{Y} = [\mathrm{Re}\{\widetilde{Y}_1\}, \mathrm{Im}\{\widetilde{Y}_1\}, \ldots, \mathrm{Re}\{\widetilde{Y}_N\}, \mathrm{Im}\{\widetilde{Y}_N\}]^T$, and analogously for $\mathbf{X}$ and $\mathbf{Z}$. We define the MIMO channel capacity as

$$C \triangleq \max_{F_{\mathbf{X}}:\, \mathrm{supp}(F_{\mathbf{X}}) \subseteq \mathcal{X}} I(\mathbf{X}; \mathbf{Y}), \tag{8}$$

where $F_{\mathbf{X}}$ is the input distribution law. The SNR definition depends on the specific constraint region $\mathcal{X}$ and it is $\mathrm{SNR} = (r_{\max}(\mathcal{X}))^2/(2N\sigma_z^2)$, with $r_{\max}(\mathcal{X}) \triangleq \sup_{\mathbf{x}\in\mathcal{X}} \{\|\mathbf{x}\|\}$.

IV. Previous Works

In [5], the authors provide capacity upper and lower bounds for AWGN MIMO systems with any channel matrix known at both the transmitter and the receiver and under an arbitrary peak amplitude constraint region $\mathcal{X}$. The resulting gap between the two bounds depends on the term $\rho = \mathrm{Vol}_{2N}(r_{\max}(\mathsf{H}\mathcal{X})\mathcal{B}_{2N}) / \mathrm{Vol}_{2N}(\mathsf{H}\mathcal{X})$, referred to as *packing efficiency* in [5]. Because of this dependence, as ρ increases, the capacity gap grows accordingly. As a result, the gap is minimized only in ideal and specific cases, for example when $\mathcal{X}$ is a ball and $\mathsf{H} = \mathsf{I}_2N$ at the same time. In [6], we improve the results of [5] for the per-antenna and total amplitude (TA) constraint, by extending the McKellips-Type upper bound of [4] to MIMO systems affected by fading. Intuitively, we achieve better results than those in [5] by considering an upper bound that depends on a smaller constraint region $\mathcal{S} \supseteq \mathsf{H}\mathcal{X}$ such that $\mathrm{Vol}_{2N}(\mathsf{H}\mathcal{X}) \leq \mathrm{Vol}_{2N}(\mathcal{S}) \leq \mathrm{Vol}_{2N}(r_{\max}(\mathsf{H}\mathcal{X})\mathcal{B}_{2N})$. Although the resulting asymptotic capacity gap in [6] is the best in the past literature, it can be far from zero, since it is given by $\log \mathrm{Vol}_{2N}(\mathcal{S}) - \log \mathrm{Vol}_{2N}(\mathsf{H}\mathcal{X})$. Moreover, as N grows larger the gap widens even more. The aim of the next section is to provide a tighter upper bound and to show that it provides an asymptotic gap equal to zero, valid for any convex constraint region.

V. Sphere Packing Upper Bound

In [7], the authors investigate the capacity of AWGN scalar channels under average and peak power constraints. They provide an upper bound based on an SP argument by using a fundamental result from convex geometry, the Steiner's formula. We extend their upper bound to MIMO fading channels. By considering an arbitrarily large number of independent channel uses, M, for $M \to \infty$, the SP bound is

$$C \leq \overline{C}_{\mathrm{SP}} \triangleq \limsup_{M\to\infty} \frac{1}{M} \log \frac{\mathrm{Vol}_n\left([\mathsf{H}\mathcal{X}]^{\times M} \oplus \delta\mathcal{B}_n\right)}{\mathrm{Vol}_n(\delta\mathcal{B}_n)} \tag{9}$$

$$= \limsup_{M\to\infty} \frac{1}{M} \log \mathrm{Vol}_n\left([\mathsf{H}\mathcal{X}]^{\times M} \oplus \delta\mathcal{B}_n\right) - \lim_{M\to\infty} \frac{1}{M} \log \mathrm{Vol}_n(\delta\mathcal{B}_n) \tag{10}$$

$$= L(\sigma_z^2) - N \log\left(2\pi e \sigma_z^2\right), \tag{11}$$

where $n = 2NM$ and $\delta = \sqrt{n\sigma_z^2}$. Let us focus on the evaluation of the term $L(\sigma_z^2)$ in (11). To deal with the convolution in (10) involving the output signal space $\mathcal{K} = [\mathsf{H}\mathcal{X}]^{\times M}$, we define the limiting normalized generating function of the intrinsic volumes of $\mathcal{K}$, $f(t)$, as follows

$$f(t) \triangleq \lim_{M\to\infty} \frac{1}{2NM} G_{\mathcal{K}}(t) \tag{12}$$

$$= \lim_{M\to\infty} \frac{1}{2NM} G_{[\mathsf{H}\mathcal{X}]^{\times M}}(t) \tag{13}$$

$$\overset{(4)}{=} \lim_{M\to\infty} \frac{M}{2NM} G_{\mathsf{H}\mathcal{X}}(t) \tag{14}$$

$$= \frac{1}{2N} \log\left(\sum_{j=0}^{2N} \mathrm{V}_j(\mathsf{H}\mathcal{X})\, e^{jt}\right). \tag{15}$$

Following the steps in [7, Lemma 14], we define $\widetilde{\mathrm{V}}_\theta(\mathcal{K}) \triangleq \widetilde{\mathrm{V}}_{j/n}(\mathcal{K}) = \mathrm{V}_j(\mathcal{K})$ with $0 \leq j \leq n$ and $\theta \in [0, 1]$. We extend one of the upper bounds of [7] to a MIMO channel by noticing that

$$\lim_{M\to\infty} \frac{1}{M} \log \widetilde{\mathrm{V}}_\theta(\mathcal{K}) = \lim_{\frac{n}{2N}\to\infty} \frac{2N}{n} \log \widetilde{\mathrm{V}}_\theta(\mathcal{K}) \tag{16}$$

$$= 2N \lim_{n\to\infty} \frac{1}{n} \log \widetilde{\mathrm{V}}_\theta(\mathcal{K}) \tag{17}$$

$$= 2N \sup_\theta \{-f^*(\theta)\}, \tag{18}$$

where (18) holds by [7, Lemma 15], which builds on the Gärtner-Ellis large deviations theorem. Let $f^*(\theta)$ be the convex conjugate of $f(t)$ defined in (5), then from [7, Theorem 8] we have

$$L(\sigma_z^2) = \limsup_{M\to\infty} \frac{1}{M} \log \mathrm{Vol}_n \left([\mathsf{H}\mathcal{X}]^{\times M} \oplus \delta\mathcal{B}_n\right) \quad (19)$$

$$\overset{(18)}{=} \sup_{\theta\in[0,1]} \left\{-2Nf^*(\theta) + (1-\theta)N\log\frac{2\pi e\sigma_z^2}{1-\theta}\right\} \quad (20)$$

$$\overset{(5)}{=} \sup_{\theta\in[0,1]} \left\{ -2N\sup_t \{\theta t - f(t)\} + (1-\theta)N\log\frac{2\pi e\sigma_z^2}{1-\theta}\right\} \quad (21)$$

$$\overset{(15)}{=} \sup_{\theta\in[0,1]} \left\{ -2N\sup_t \left\{\theta t - \frac{1}{2N}\log\left(\sum_{j=0}^{2N} \mathrm{V}_j\left(\mathsf{H}\mathcal{X}\right)e^{jt}\right)\right\} + (1-\theta)N\log\frac{2\pi e\sigma_z^2}{1-\theta}\right\}. \quad (22)$$

Finally, by plugging (22) into (11) we derive the final bound.

A. Asymptotic Gap

Let us now evaluate the asymptotic tightness of the gap between the SP bound $\overline{C}_{\text{SP}}$ and the entropy power inequality (EPI) lower bound, which is derived in [5] as

$$\underline{C}_{\text{EPI}} = N\log\left(1 + \frac{\mathrm{Vol}_{2N}\left(\mathsf{H}\mathcal{X}\right)^{\frac{1}{N}}}{2\pi e\sigma_z^2}\right). \quad (23)$$

Since in the interval $[0,\infty)$ the function $L(\sigma_z^2)$ is continuous [7], and since $\mathrm{Vol}_n\left([\mathsf{H}\mathcal{X}]^{\times M}\right) = M\mathrm{Vol}_{2N}\left(\mathsf{H}\mathcal{X}\right)$, it holds

$$\lim_{\sigma_z^2\to 0} L(\sigma_z^2) = L(0) = \limsup_{M\to\infty}\frac{1}{M}\log\mathrm{Vol}_n\left([\mathsf{H}\mathcal{X}]^{\times M}\right) \quad (24)$$

$$= \log\mathrm{Vol}_{2N}\left(\mathsf{H}\mathcal{X}\right). \quad (25)$$

The gap at high SNR results in

$$g_a \triangleq \lim_{\sigma_z^2\to 0} \overline{C}_{\text{SP}} - \underline{C}_{\text{EPI}} \quad (26)$$

$$= \lim_{\sigma_z^2\to 0} L(\sigma_z^2) - N\log\left(\mathrm{Vol}_{2N}\left(\mathsf{H}\mathcal{X}\right)^{\frac{1}{N}}\right) = 0. \quad (27)$$

Therefore, we proved that the SP upper bound is asymptotically tight at high SNR for any dimension N of the MIMO system, any channel matrix H, and any convex constraint region $\mathcal{X}$. In the following section, we refine and investigate the bounding gap as a function of the SNR for the TA constraint.

VI. Total Amplitude Constraint

We evaluate the SP upper bound of Sec. V for the input constraint region $\mathcal{X} = a\mathcal{B}_{2N}$. The TA constraint occurs, for instance, when the transmitter employs a single amplifier for all of the transmitting antennas. As shown in (22), to evaluate the bound we need to compute the intrinsic volumes $\mathrm{V}_j\left(\mathsf{H}\mathcal{X}\right)$, for $j = 0,\dots,2N$. Since $\mathcal{X}$ is a ball, and by using the singular value decomposition of $\mathsf{H} = \mathsf{U}\mathsf{\Lambda}\mathsf{V}^T$, it holds $\mathrm{V}_j\left(\mathsf{H}\mathcal{X}\right) = \mathrm{V}_j\left(\mathsf{\Lambda}\mathcal{X}\right)$, for any j. We denote the diagonal elements of $\mathsf{\Lambda}$ as $\lambda_1,\dots,\lambda_{2N}$ and we assume that $\lambda_1 \geq \lambda_2 \geq \cdots \geq \lambda_{2N}$,

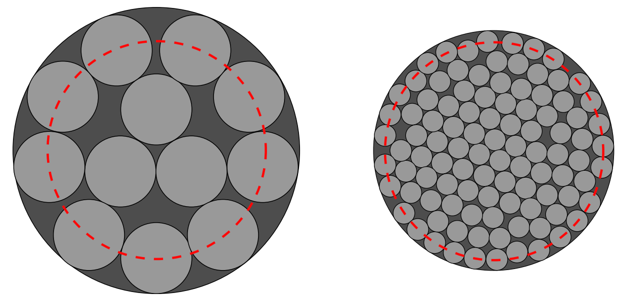

Figure 1. Two sphere packing examples under a peak amplitude constraint and different SNR values. For both figures, the red dashed line is the border of $\mathcal{K} = \mathcal{B}_2$, in dark gray the result of the Minkowski sum between $\mathcal{K}$ and the noise ball for each specific SNR. On the left, the light gray noise balls are translated replicas of $\delta_1\mathcal{B}_2$, while on the right of $\delta_2\mathcal{B}_2$ with $\delta_1 > \delta_2$.

since it is always possible to rearrange the MIMO system in such a way that this condition is satisfied. In [9], it is shown that given an ellipsoid

$$\mathcal{E} = \left\{\mathbf{x} = [x_1,\dots,x_{2N}]^T \in \mathbb{R}^{2N} : \mathbf{x}^T\mathbf{\Sigma}^{-1}\mathbf{x} \leq 1\right\}, \quad (28)$$

by defining j independent and identically distributed random vectors $\mathbf{Q}_1,\dots,\mathbf{Q}_j \sim \mathcal{N}\left(\mathbf{0}_{2N},\Sigma\right)$ and the random matrix $\mathsf{Q} = [\mathbf{Q}_1,\dots,\mathbf{Q}_j]$, it is possible to compute the jth intrinsic volume of $\mathcal{E}$ as

$$\mathrm{V}_j\left(\mathcal{E}\right) = \frac{(2\pi)^{j/2}}{j!}\mathsf{E}\left[\sqrt{\det\left(\mathsf{Q}^T\cdot\mathsf{Q}\right)}\right]. \quad (29)$$

Let us set $\Sigma = \Lambda^2$. Then, the intrinsic volumes for the TA configuration are given by

$$\mathrm{V}_j\left(\mathsf{H}\mathcal{X}\right) = \mathrm{V}_j\left(\mathcal{E}\right)a^j, \qquad j = 0,\dots,2N. \quad (30)$$

By plugging the intrinsic volumes (30) into (22), we obtain the TA upper bound on the capacity.

Although the SP upper bound is asymptotically tight, it can be loose at low-to-intermediate SNR. Indeed, since the SP bound is based on geometric arguments, its reliability depends on how accurately the Minkowski sum approximates the true channel output region. Intuitively, the Minkowski sum in (9) is obtained by taking the union of the noise balls $\delta\mathcal{B}_n$ centered on each point in $\mathcal{K} = [\mathsf{H}\mathcal{X}]^{\times M}$. Conversely, a true sphere packing problem would take the union of non-overlapping replicas of $\delta\mathcal{B}_n$, filling $[\mathsf{H}\mathcal{X}]^{\times M} \oplus \delta\mathcal{B}_n$. Therefore, as the noise balls get smaller, the Minkowski sum becomes a good approximation of the output signal space $[H\mathcal{X}]^{\times M}$, as shown in Fig. 1. Nonetheless, whenever it is possible to decompose the constraint in separate independent contributions on different MIMO subspaces, we can obtain a family of SP bounds that improves upon the one proposed in Sec. V. Specifically, we can separate the MIMO channel into two independent subchannels: we apply the SP upper bound on one and the Gaussian maximum-entropy property on the other. Given the MIMO channel capacity

$$C = \max_{F_{\mathbf{X}}:\|\mathbf{X}\|\leq a} \{\mathsf{h}\left(\mathbf{Y}\right)\} - \mathsf{h}\left(\mathbf{Z}\right), \quad (31)$$

an upper bound on the first term is given by

$$\max_{F_{\mathbf{X}}:\|\mathbf{X}\|\leq a}\{\mathsf{h}(\mathbf{Y})\} = \max_{F_{\mathbf{X}}:\|\mathbf{X}\|\leq a}\{\mathsf{h}(\mathbf{Y}_u,\mathbf{Y}_l)\} \tag{32}$$

$$\leq \max_{F_{\mathbf{X}}:\|\mathbf{X}\|\leq a}\{\mathsf{h}(\mathbf{Y}_u)+\mathsf{h}(\mathbf{Y}_l)\}, \tag{33}$$

where $\mathbf{Y}=[\mathbf{Y}_u,\mathbf{Y}_l]^T$, with $\mathbf{Y}_u=[Y_1,\ldots,Y_U]^T\in\mathbb{R}^U$, and $\mathbf{Y}_l=[Y_{U+1},\ldots,Y_{U+L}]^T\in\mathbb{R}^L$, and $U+L=2N$. We want to treat independently the contributions of $\mathsf{h}(\mathbf{Y}_u)$ and $\mathsf{h}(\mathbf{Y}_l)$, to upper bound them with different techniques. Since we assumed that the singular values of Λ are sorted in descending order, the subsystem to which $\mathbf{Y}_u$ belongs perceives larger singular values, and therefore higher SNR. On the contrary, $\mathbf{Y}_l$ refers to the subsystem with smaller singular values and affected by a lower SNR. Then, we expect the SP upper bound to be tighter on $\mathsf{h}(\mathbf{Y}_u)$, where the transmitted signal is stronger compared to the noise level, while we expect it to be looser on $\mathsf{h}(\mathbf{Y}_l)$. Since in the subsystem of $\mathbf{Y}_l$ the Gaussian noise is dominant, a tighter upper bound on $\mathsf{h}(\mathbf{Y}_l)$ can be provided by the differential entropy of a normally distributed vector $\overline{\mathbf{Y}}_l\sim\mathcal{N}(\mathbf{0}_{2N},\Sigma_l)$, with $\Sigma_l=\Lambda_l\mathsf{E}\left[\mathbf{X}_l\mathbf{X}_l^T\right]+\sigma_z^2\mathsf{I}_L$ and with Λ_l being the $L\times L$ submatrix of Λ with diagonal elements $\lambda_{U+1},\ldots,\lambda_{2N}$. Finally, to separate the capacity contributions of the two subsystems, we need to reformulate the input constraint in such a way that it can be separated as well. Since

$$\|\mathbf{X}\|^2=\|\mathbf{X}_u\|^2+\|\mathbf{X}_l\|^2\leq a^2, \tag{34}$$

we can reinterpret a^2 as $a^2(1-\rho)+a^2\rho$ with $\rho\in[0,1]$. Therefore, the constraint $\|\mathbf{X}\|\leq a$ becomes equivalent to

$$\begin{cases}\|\mathbf{X}_u\|\leq a\sqrt{1-\rho}\\ \|\mathbf{X}_l\|\leq a\sqrt{\rho}.\end{cases} \tag{35}$$

Plugging this equivalent constraint into (33), we obtain

$$\max_{F_{\mathbf{X}}:\|\mathbf{X}\|\leq a}\{\mathsf{h}(\mathbf{Y}_u)+\mathsf{h}(\mathbf{Y}_l)\} \tag{36}$$

$$=\max_{\rho\in[0,1]}\left\{\max_{F_{\mathbf{X}}:\begin{cases}\|\mathbf{X}_u\|\leq a\sqrt{1-\rho}\\ \|\mathbf{X}_l\|\leq a\sqrt{\rho}\end{cases}}\{\mathsf{h}(\mathbf{Y}_u)+\mathsf{h}(\mathbf{Y}_l)\}\right\} \tag{37}$$

$$=\max_{\rho\in[0,1]}\left\{\max_{F_{\mathbf{X}_u}:\|\mathbf{X}_u\|\leq a\sqrt{1-\rho}}\{\mathsf{h}(\mathbf{Y}_u)\} + \max_{F_{\mathbf{X}_l}:\|\mathbf{X}_l\|\leq a\sqrt{\rho}}\{\mathsf{h}(\mathbf{Y}_l)\}\right\}. \tag{38}$$

Then, we can apply the SP upper bound in (9) on the subsystem of $\mathbf{Y}_u$ to get

$$\max_{F_{\mathbf{X}_u}:\|\mathbf{X}_u\|\leq a\sqrt{1-\rho}}\{\mathsf{h}(\mathbf{Y}_u)\}\leq L_u(\rho) \tag{39}$$

$$=\sup_{\theta\in[0,1]}\left\{-U\sup_t\left\{\theta t-\frac{1}{U}\log\sum_{j=0}^{U}\mathrm{V}_j(\Lambda_u\mathcal{X}_u)\,e^{jt}\right\} + (1-\theta)\frac{U}{2}\log\frac{2\pi e\sigma_z^2}{1-\theta}\right\}, \tag{40}$$

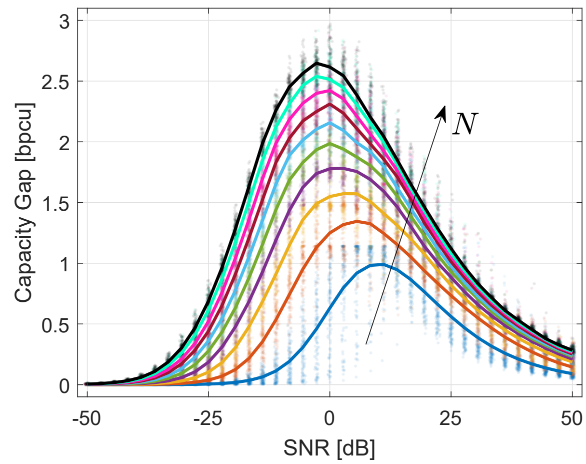

Figure 2. Numerical evaluation of the capacity gap in bit per channel use (bpcu) versus SNR, for $N=1,\ldots,10$. For each N the filled circles are the gaps resulting from each random channel realization, while the solid lines show the averaged behavior.

where $\mathcal{X}_u=a\sqrt{1-\rho}\mathcal{B}_U$, and Λ_u is the $U\times U$ submatrix of Λ with diagonal elements $\lambda_1,\ldots,\lambda_U$. For the subsystem associated with $\mathbf{Y}_l$, the upper bound is given by

$$\max_{F_{\mathbf{X}_l}:\|\mathbf{X}_l\|\leq a\sqrt{\rho}}\{\mathsf{h}(\mathbf{Y}_l)\}\leq\max_{F_{\mathbf{X}_l}:\|\mathbf{X}_l\|\leq a\sqrt{\rho}}\{\mathsf{h}(\overline{\mathbf{Y}}_l)\} \tag{41}$$

$$=\max_{\substack{\mathsf{E}[|\mathbf{X}_l|^2]:\\ \|\mathbf{X}_l\|\leq a\sqrt{\rho}}}\sum_{j=U+1}^{2N}\frac{1}{2}\log\left(2\pi e\left(\lambda_j^2\rho\mathsf{E}\left[|X_j|^2\right]+\sigma_z^2\right)\right) \tag{42}$$

$$=\sum_{j=U+1}^{2N}\frac{1}{2}\log\left(2\pi e\left(\lambda_j^2\rho P_j+\sigma_z^2\right)\right), \tag{43}$$

where P_j is the power allocation given by the water-filling algorithm, which maximizes (42) for the given constraint $\|\mathbf{X}_l\|\leq a\sqrt{\rho}$. Notice that we obtain a valid upper bound for any combination of positive integers U and L with sum equal to $2N$, therefore the final upper bound for the TA configuration results in

$$C\leq\overline{C}_{\mathrm{TA}}=\min_{\substack{U:\\ U+L=2N}}\max_{\rho}\left\{L_u(\rho)+\sum_{j=U+1}^{2N}\frac{1}{2}\log\left(2\pi e\left(\lambda_j^2\rho P_j+\sigma_z^2\right)\right)\right\} - N\log(2\pi e\sigma_z^2). \tag{44}$$

To evaluate the gap we consider the piecewise-EPI (p-EPI) lower bound proposed in [6] and we denote it with $\underline{C}_{\mathrm{TA}}$. Let us define the gap as $g\triangleq\overline{C}_{\mathrm{TA}}-\underline{C}_{\mathrm{TA}}$. We evaluate g numerically by Monte Carlo simulation for $N=1,\ldots,10$, where the entries of $\widetilde{\mathsf{H}}$ in (6) are drawn as $\widetilde{H}_{i,j}\sim\mathcal{CN}(0,2),\ \forall i,j$. The results are presented in Figs. 2 and 3. In Fig. 2, we show a scatter plot of the gap realizations and the average gap versus SNR, for any N. As expected, when the SNR goes to

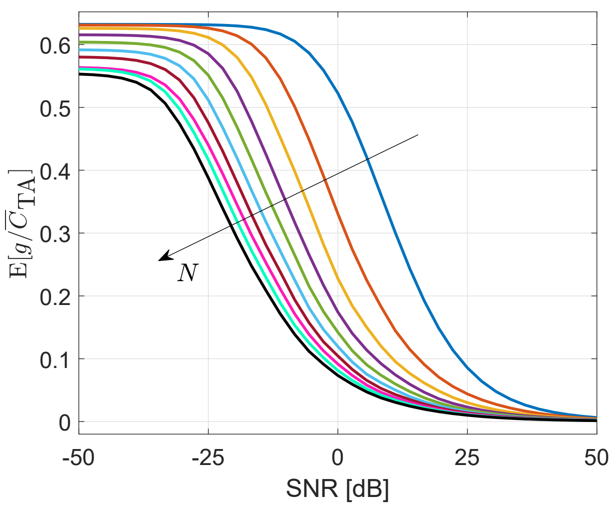

Figure 3. Numerical evaluation of the average ratio between the capacity gap g and the upper bound $\overline{C}_{\mathrm{TA}}$ versus SNR, for $N = 1, \ldots, 10$.

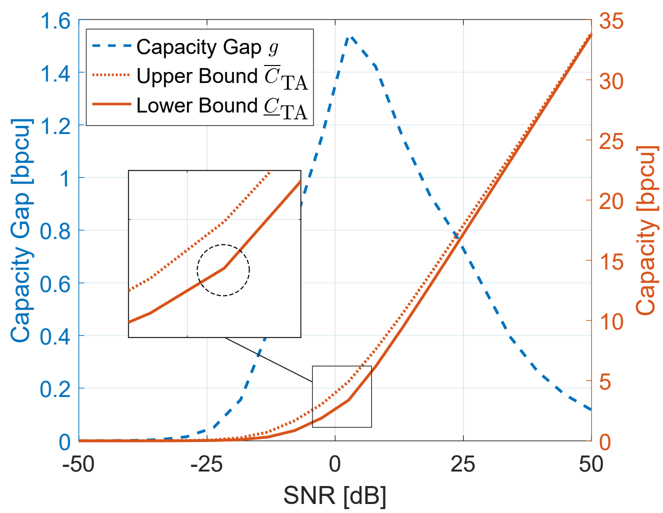

Figure 4. Capacity gap (dashed blue curve) and capacity bounds (dotted and solid red curves) vs SNR. The channel realization $\widetilde{\mathsf{H}}$ has singular values $\widetilde{\boldsymbol{\lambda}} = [2.6, 0.9]$.

zero the gap is small, because (44) is optimized by $U = 0$ and $\overline{C}_{\mathrm{TA}}$ turns into the Gaussian maximizing entropy bound, which is tight at low SNR. Moreover, the gap is vanishing at high SNR as proven in Section V. Even in the worst case, g is ~ 3 bit per channel use (bpcu) and it moderately increases with N. In fact, in Fig. 3 we show that as N increases, the ratio between the bounding gap and the upper bound decreases and, therefore, that the bounds provide a proportionally more accurate estimate of the channel capacity for larger values of N. The curves shown in Fig. 2 are smooth and regular due to averaging. On the contrary, the gap curve for a single channel matrix typically exhibits a much more irregular trend, with a number of spikes increasing with N. For instance, the gap shown in Fig. 4 for $N = 2$ presents a spike around $\mathrm{SNR} = 2.5$ dB. This trend is due to the piecewise nature of the p-EPI lower bound in [6], which produces discontinuities in the lower bound curve and consequently affects the resulting gap as well. Such an effect becomes more evident when the singular values of H are strongly dissimilar.

VII. Conclusion

We derived an upper bound on the channel capacity of multiple-input multiple-output (MIMO) systems affected by fading and subject to amplitude constraints at the transmitter, that is asymptotically tight at high signal-to-noise ratio (SNR) for any channel matrix realization, any peak amplitude convex constraint region, and any dimension of the MIMO system. Moreover, for a specific scenario where the total input power of the MIMO system is peak-constrained, we refined the capacity upper bound and evaluated numerically the bounding gap for a broad range of SNR levels.

References

[1] J. G. Smith, "The information capacity of amplitude- and variance-constrained scalar Gaussian channels," *Information and Control*, vol. 18, no. 3, pp. 203–219, April 1971.

[2] S. Shamai and I. Bar-David, "The capacity of average and peak-power-limited quadrature Gaussian channels," *IEEE Transactions on Information Theory*, vol. 41, no. 4, pp. 1060–1071, July 1995.

[3] B. Rassouli and B. Clerckx, "On the capacity of vector Gaussian channels with bounded inputs," *IEEE Transactions on Information Theory*, vol. 62, no. 12, pp. 6884–6903, December 2016.

[4] A. Thangaraj, G. Kramer, and G. Böcherer, "Capacity bounds for discrete-time, amplitude-constrained, additive white Gaussian noise channels," *IEEE Transactions on Information Theory*, vol. 63, no. 7, pp. 4172–4182, July 2017.

[5] A. Dytso, M. Goldenbaum, S. Shamai, and H. V. Poor, "Upper and lower bounds on the capacity of amplitude-constrained MIMO channels," in *GLOBECOM 2017 - 2017 IEEE Global Communications Conference*, December 2017, pp. 1–6.

[6] A. Favano, M. Ferrari, M. Magarini, and L. Barletta, "Capacity bounds for amplitude-constrained AWGN MIMO channels with fading," in *2020 IEEE International Symposium on Information Theory (ISIT)*, August 2020, pp. 2032–2037.

[7] V. Jog and V. Anantharam, "A geometric analysis of the AWGN channel with a (σ, ρ)-power constraint," *IEEE Transactions on Information Theory*, vol. 62, no. 8, pp. 4413–4438, August 2016.

[8] M. Lotz, M. B. McCoy, I. Nourdin, G. Peccati, and J. A. Tropp, "Concentration of the intrinsic volumes of a convex body," in *Geometric Aspects of Functional Analysis*. Springer, July 2020, pp. 139–167.

[9] D. Zaporozhets and Z. Kabluchko, "Random determinants, mixed volumes of ellipsoids, and zeros of Gaussian random fields," *Journal of Mathematical Sciences*, vol. 199, no. 2, pp. 168–173, May 2014.